Buckling Optimization of Composite Panels with Curvilinear Fibers and Grid Stiffeners

Sofía Arranz Hernando
sofia.arranz.hernando@tecnico.ulisboa.pt

Instituto Superior Técnico, Universidade de Lisboa, Portugal

September 2021

Abstract

Automated Fiber Machines (AFP) can manufacture composite panels with curvilinear fibers. The stiffness of the panel depends on the spatial location. This can be tailored to improve the structural performance. In this work, the buckling performance of composite panels with curvilinear fibers and grid stiffeners is optimized using a genetic algorithm. To this end, the objective is to maximize the critical buckling load. The skin is composed of layers in which the fiber orientation varies along one spatial direction. Two design variables define each unique layer: the fiber angle at the center and side of the panel. The stiffener layout is parametrized by other two design variables, which are the stiffener location and its curvature. Manufacturing constraints in terms of maximum curvature allowable by the AFP machine are imposed for both skin and stiffener fibers. The effect of manufacturing-induced gaps in the laminates is also incorporated. The finite element method is used to perform the buckling analyses. The skin is modeled with shell elements and the stiffeners are idealized by beam elements. The panels are subjected to in-plane compressive loads and shear loads under several boundary conditions. Optimization results show the use of curvilinear fibers for both skin and stiffeners can increase the buckling load. The improvement over the straight fiber design depends on the load case and boundary conditions. The optimization framework developed can help the designer to evaluate in which scenarios grid-stiffened curvilinear fiber composite panels provide the greatest benefit for the critical buckling load.

Keywords: Variable Stiffness Composite Structures, Curvilinearly Grid-stiffened panels, Manufacturing Constraints, Buckling, Finite element analysis, Optimization.

1. Introduction

The main driver in the development of materials for aerospace structures is weight reduction. Weight savings mean less fuel is required, which in turn results in a higher payload capacity or a longer range of the aircraft. The call for weight reduction in the aerospace industry has led to the increasing use of composite materials due to their high specific strength and stiffness. Traditionally, composites are made of straight fibers. Recent advances in manufacturing technology, such as Automated Fiber Placement (AFP) machines, have made it possible to steer the fibers. Laminates composed of plies in which the fiber orientation continuously varies can be manufactured. It is also feasible to manufacture curvilinearly grid-stiffened panels for enhanced structural performance. The stiffness of those composite panels is, therefore, not constant and depends on the spatial location. The design space is enlarged and substantial improvements in structural performance or weight savings can be obtained. These panels can be employed to manufacture wing or fuselage skins. Skins are thin-walled structures subjected to in-plane loads and are prone to buckling. Hence, this work focuses on the buckling performance of composite panels with curvilinear fibers and grid stiffeners and aims to answer to what extent tailoring the stiffness variation can increase the buckling load.

In the literature, different approaches have been adopted to define the fiber paths of Variable Stiffness (VS) laminates. Olmedo and Gürdal [1] introduced the linear variation of the fiber angle along one spatial direction to describe curvilinear fiber paths. Improvements in the buckling load of up to 80% over straight fiber laminates were found. Wu et al. [2] defined the fiber angles based on a nonlinear distribution and applied the Rayleigh–Ritz method to perform the buckling analysis of VS panels. S. Ijsselmuiden [3] employed lamination parameters to describe the structural stiffness of VS laminates. This approach decreased the number of design variables, however, a postprocessing step was necessary to convert the optimal lamination parameters into continuous fiber paths

When manufacturing a variable stiffness laminate by AFP machine, gaps and overlaps are induced. The study of the influence of those defects on the laminate structural performance has attracted the interest of many authors. A.Blom et al. [4] developed a FE model in which the elements were assumed to be either in 'regular' composite zones or in gap zones (characterized by resin properties). It was concluded that a larger gap area decreased the laminate strength and stiffness. Fayazbakhsh et al. [5] modeled VS laminates with embedded defects

by computing the percentage of the defect area within an element. The gap area was used to scale the material properties while the overlap area scaled the thickness. In their work, the results showed that gaps degraded in-plane stiffness and buckling load while overlaps improved them. T.Brooks et al. [6] linked the gap/overlap propagation rate and the divergence of a 2D vector field. A positive divergence implied gap formation, while a negative value indicated overlap formation.

Curvilinearly grid-stiffened layouts can also increase the buckling load of the panel. Several authors [7, 8, 9, 10], used the linear variation of the fiber angle to define the stiffener paths. The stiffness distribution of the panel was influenced by the angle variation and the distance between the stiffeners. Kapania and his co-authors [11, 12, 13] employed NURBS (Non-Uniform Rational B-Splines) to describe the reference path of curvilinear stiffeners. It was shown that curvilinear stiffeners could result in a better design than straight stiffeners, but not for all load cases and boundary conditions. Other authors [14, 15] parametrized the stiffener geometry using Bézier curves. For NURBS and Bézier curves, special attention was required to ensure that the stiffener lied within the panel boundary.

Designing the optimum staking sequence or the optimum stiffener layout and size often results in many local optima [12, 16]. In addition, the sensitivity information of the problem is not always easy to compute. Hence, global optimization techniques are required. Genetic algorithms (GA) are the most widely adopted for the buckling optimization of VS laminates and/or curvilinearly grid-stiffened panels (see, for instance [2, 17, 18]).

In this paper, an optimization framework has been developed with the aim of designing composite panels with curvilinear fibers and curvilinear stiffeners for maximum buckling performance. Manufacturing constraints in terms of the maximum allowed curvature by the AFP machine have been imposed for both the skin and stiffener fibers. Manufacturing-induced defects in the form of gaps have been also considered in the design phase. Panels under several boundary conditions and load cases have been optimized using Genetic Algorithm.

2. Numerical Modeling

2.1. Curvilinear Skin Fibers

The linear variation of the fiber angle, first introduced by Olmedo and Gürdal [1], has been widely employed to study VS panels due to its simplicity and robustness, and is therefore the approach adopted. In the present work, the fiber angle varies along the x-direction according to Eq.1:

$$\theta(x) = (T_1 - T_0)\,\frac{|x|}{a} + T_0 \qquad (1)$$

where T_0 and T_1 are the fiber angles at the start and end of the characteristic length a; a is considered here as the half side of the square panel. Figure 1 schematized the terms of Eq.1.

At each x-position of the VS ply, the fiber angle is different. The skin is meshed with a suitable number of

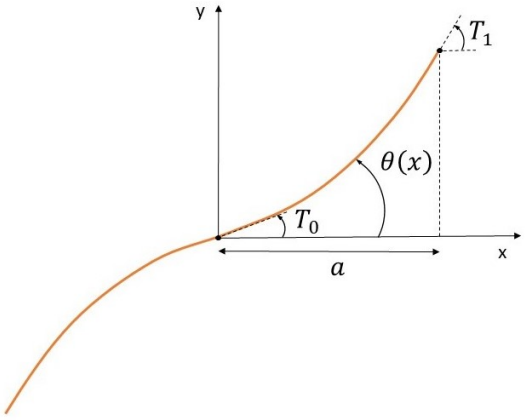

Figure 1: Reference path defined by the the linear variation of the fiber angle

elements to account for the variation of the fiber angle, i.e., the stiffness. Four-node shell (S4R) elements are used. At the centroid of each element, the fiber angle is computed with Eq.1. Since Eq.1 depends on T_0 and T_1, the variables that characterize a ply, a fiber angle is obtained for each different ply in the laminate.

The local stacking sequence is then built and assigned to the element. As a result, there are as many composite sections as there are elements. In this way, a variable stiffness composite panel with an arbitrary ply configuration can be modeled.

Figure 2a illustrates the fiber paths for a $\langle 20, 50\rangle$ ply. Figure 2b shows how the fiber paths of the ply are discretized in the FE model. The straight lines represent the fiber angle computed at the centroid of each element.

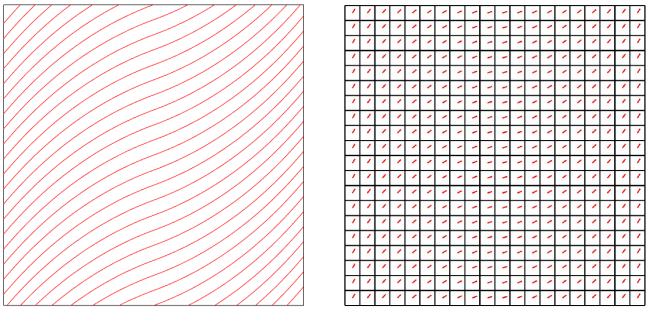

(a) Continuous fiber paths (b) Fiber angle in elements

Figure 2: Modelling of tow steered $\langle 20, 50\rangle$ ply

The Abaqus-Python script developed for VS laminate modeling has been validated with the study presented by Waldhart [19]. The buckling loads for VS laminates were obtained and compared to those reported by the author. The percent error was less than 1%.

2.2. Modeling of Manufactured-induced Gaps

Shifted method is used to manufacture variable-stiffness laminates. First, the AFP machine deposits the reference course. The distance between the top and bottom boundaries of the course changes along the horizontal di-

rection since the fiber path is curvilinear. The AFP head moves in the vertical direction with a constant value to lay down the next course. If the course width remains constant, large areas of overlap will occur between both courses. Therefore, the course width should vary continuously. This variation is actually discrete, as the AFP can only cut finite tow widths. Small areas of defects are then generated.

The defects generated can be gaps or overlaps. A gap is a small wedge-shaped without fibers which, after curing, will be filled with resin. An overlap occurs when a small jagged patch of the composite tow lies on top of the adjacent composite course. The 100% coverage or complete overlap strategy has been shown to provide increased structural performance, however, the laminate thickness is not constant. Many aeronautical applications require a smooth surface to maintain aerodynamics, which will not be possible to manufacture with the overlap strategy [5]. Therefore, in this work, 0% coverage or complete gap strategy has been chosen.

One-sided tow drop technique is employed to cut the tows. It implies that one course boundary, either the top or the bottom one, is cut and the other remains smooth.

The approach introduced by Fayazbakhsh et al. [5], called the Defect Layer Method, has been modified to consider the induced gaps when the linear variation of the fiber angle is used to define the fiber paths. A MATLAB code has been developed to locate the gaps in the laminate and obtain their area. Next, the Python script builds the FE model of the VS laminate with embedded gaps. Hereafter, the basics of the code are explained.

When the AFP machine deposits the course, its head is perpendicular to the local fiber angle. This means that each point along the AFP head has the same orientation as the one corresponding to the reference path. Thus, the points that form each tow of the course can be calculated by Eq.2.

$$\begin{aligned} x &= x^* - i \cdot t_w sin\theta^* \\ y &= y^* + i \cdot t_w cos\theta^* \end{aligned} \tag{2}$$

where t_w is the tow width and n_t the number of tows in a course. The superscript $*$ is used to denote the points in the reference path and i is an index which range decreases by 1 from $n_t/2$ to $-n_t/2$.

The shift distance, i.e., the minimum vertical distance between the top and bottom boundaries of the reference course, is calculated as shown in Eq. 3.

$$d_s = min\left(\frac{n_t t_w}{cos\theta^*}\right) \tag{3}$$

The AFP machine will move vertically with the shift distance to lay down the next course (the shifted course). The points of the shifted course can be obtained by Eq.4 .

$$\begin{aligned} x_s &= x^* - i \cdot t_w sin\theta^* \\ y_s &= y^* + i \cdot t_w cos\theta^* + d_s \end{aligned} \tag{4}$$

The intersections between the outer top edge of the reference course and the tows of the shifted course are next located. A perpendicular line is drawn from each intersection point up to the next corresponding tow edge, reproducing the tow cut made by the AFP machine. The geometry of the gaps is generated. Figure 3a shows the intersection points between the shifted course and the reference course. Figure 3b depicts the gap set generated due to that intersection.

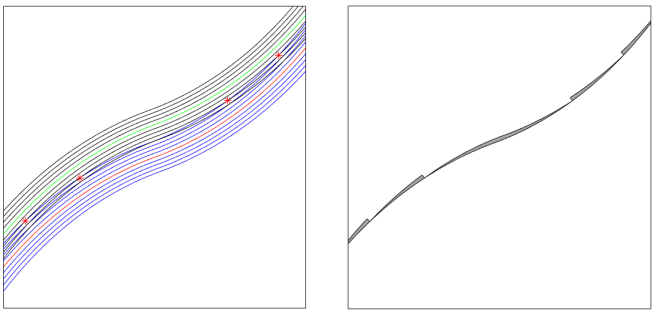

(a) Intersection points (b) Gaps formation

Figure 3: Intersection between the shifted course and the reference course

The distance between two sets of gaps is the shift distance and, thus, the gap set is translated vertically to generate the defects across the entire ply. The gap distribution is then intersected with the skin mesh to calculate the gap area within an element. Figure 4a illustrates the intersection between the skin mesh and the gaps generated in the ply.

The gaps are resin rich areas, so a higher value of gap area means impoverishing the material properties of the laminate. The 'modified' rule of mixtures (Eqs. 5 - 8) is used to scale the elastic properties of each element according to the gap area fraction. The gap area fraction is defined as the value of the gap area in each element divided by the area of the mesh element.

$$E_1 = A_c E_{1c} + A_m E_m \tag{5}$$

$$E_2 = \frac{E_{2c} E_m}{A_m E_{2c} + A_c E_m} \tag{6}$$

$$G_{12} = \frac{G_{12c} G_m}{A_m G_{12c} + A_c G_m} \tag{7}$$

$$G_{23} = A_c G_{23c} + A_m G_m \tag{8}$$

$$\nu_{12} = A_c \nu_{12c} + A_m \nu_m \tag{9}$$

The subscript c represents the non-defective composite and the subscript m the matrix or gaps. The composite area fraction, A_c, and the gap area fraction, A_m, are equivalent to the volume fraction since the thickness ply is the same with or without gaps. Obviously, $A_c = 1 - A_m$. Figure 4b shows the resulting scaled materials.

Note that the gap formation varies depending on the fiber angles T_0 and T_1. This implies that the gap areas and the corresponding material properties are calculated for each different ply of the laminate. The scaled material properties are used then to build the FE model, creating a material for each ply and element.

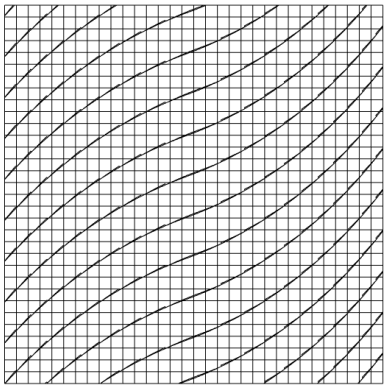

(a) Intersection between the mesh of the skin and the gap distribution

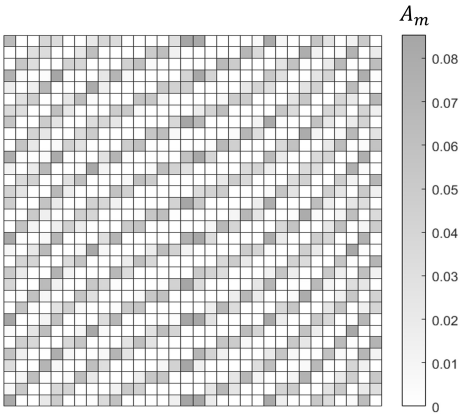

(b) Scaled material properties according to gap area

Figure 4: Modeling of the gap distribution generated in a ply

The study presented by Fayazbakhsh et al. [5] was reproduced to validate the present gap module. The authors defined the curvilinear fibers by a constant curvature path, whereas in the present work the linear variation of the fiber angle is used. Although the fiber path definition influences on the gap formation, the buckling load reported by Fayazbakhsh et al. and that obtained by the present model differ by less than 5%. Hence, the model developed is considered to capture correctly the effect of gaps.

2.3. Curvilinear Stiffeners

The parametrization presented by [11, 12, 13] has been modified to characterize the stiffener geometry. The stiffener curvilinear path is modeled by a cubic spline with 3 control points. The following assumptions have been made to reduce the number of design variables of the stiffener layout. Four symmetrical stiffeners are attached to the skin. Thus, it is sufficient to define the geometry of one stiffener. The start point of the stiffener, A, is located at the bottom edge of the plate. The end point, B, is placed at the plate upper edge on the same vertical as the start point.

Consequently, the stiffener layout is governed by two design variables: ε and α. The ε parameter is defined on the plate boundary and varies from 0 to 1, where 1 is the whole perimeter. It controls the stiffener location. The α parameter is the normalized distance to the midpoint C. It controls the stiffener shape. Although this approach is quite simple, it allows a reduced number of design variables and facilitates to control that the stiffeners lie inside the panel. The choice of appropriated bounds for the design variables is also easier. Figure 5a illustrates the stiffener layout that is considered in this work.

Note that the stiffener could also be modeled directly by the coordinates of the points, resulting in four design variables. However, this geometry parameterization, in its most general form, requires three design variables $(\varepsilon_A, \varepsilon_B, \alpha)$ and is, therefore, applied.

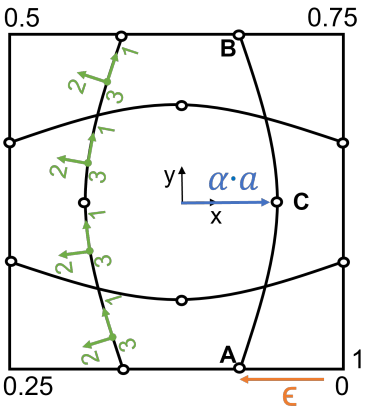

(a) Stiffener layout

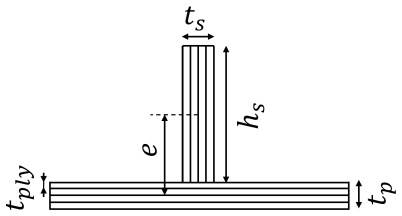

(b) Cross-section of the panel

Figure 5: Schemes of the composite panel with curvilinear stiffeners

Once the stiffener path is parameterized, its cross section is defined. The AFP machine successively places one tow on top of another to manufacture the stiffeners. This results in a rectangular stiffener cross-section, described by two dimensions: the stiffener thickness, t_s, and the stiffener height, h_s. The stiffeners are modeled by 2-node linear beam element (B31, Timoshenko beam).

The stiffener laminate is assumed to be perpendicular to the plate midplane. In addition, the strong direction of the material is set to be coincident with the longitudinal direction of the stiffener. This simulates that the fibers are aligned with the local orientation of the stiffeners, i.e, the fibers follow the stiffener path, as it can be seen in Figure 5a. Thus, the stiffeners are modeled with a zero angle laminate. The zero angle fiber ply in the stiffener is shown to provide a larger bending stiffness to the plate, enhancing the structural stability of the design [11].

The stiffeners are attached eccentrically to the plate. The stiffener eccentricity is defined in Eq.10 as the offset between the stiffener centroid and the panel midplane [11].

$$e = \frac{1}{2}\left(h_s + t_p\right) \tag{10}$$

Figure 5b indicates the dimensions of cross-sectional view of the panel.

Abaqus' built-in *tie constraint* has been used to attach the stiffeners to the plate. The *tie constraint* ties two separate surfaces together so that there is no relative motion between them [20]. Its major advantage is that it allows fusing together a pair of regions with dissimilar meshes, as it is the case here. Therefore, it is not necessary for the stiffener nodes to coincide with the plate nodes, which reduces the complexity of the setup.

Zhao et al.[21] studied the buckling behaviour of a curvilinearly grid-stiffened panel. This work has been employed to validate the Python script developed to model curvilinear stiffeners. The percent error between the buckling load reported by Zhao et al. and that obtained by the present model was less than 2%.

3. Optimization Statement

Genetic Algorithm (GA) is employed as the optimizer. In this work, the optimization process has been implemented in MATLAB. The objective of the optimization is to maximize the buckling load of VS composite panels with curvilinear stiffeners. To this end, the objective function, f, to be minimized is the inverse of the normalized buckling factor, $\overline{BF}$. The buckling factor is defined as the ratio of the buckling load and the applied load. The buckling factor is normalized to the buckling factor of the first evaluation of the objective function.

The design variables, $\mathbf{x}$, can be divided into two sets: those of the skin fibers and those of the stiffener layout. To define the path of the skin fibers according to Eq.1, two fiber angles and a characteristic length are needed. The present work considers the plate dimensions fixed and the fiber angles as the design variables. Therefore, there will be two design variables for each different ply of the laminate: T_0^i and T_1^i. Two different plies are considered, resulting in four design variables for the skin laminate: $T_0^1, T_1^1, T_0^2, T_1^2$. As described in Section 2.3, the stiffener layout is determined by the ε location parameter and the α shape parameter, which constitute the other two design variables. Hence, a total of six design variables define the problem, which makes the optimization using GA affordable in computational time.

The manufacturing constraints, g, in terms of maximum curvature allowable by the AFP machine are imposed for both skin and stiffener fibers. Section 3.1 explains how the curvature of the skin and stiffener fibers is computed.

The optimization formulation for the design problem can be expressed as:

$$\begin{aligned} \text{Minimize} \quad & f = \frac{1}{\overline{BF}} \\ \text{w.r.t.} \quad & \mathbf{x} = \left[T_0^i, T_1^i, \varepsilon, \alpha\right] , \\ \text{subject to} \quad & g_i = \frac{\left|\kappa^i_{max,f}\right|}{\kappa_{AFP}} - 1 \leq 0 \quad \text{for} \quad i = 1, 2, ..., m, \\ & g_{i+1} = \frac{|\kappa_{max,s}|}{\kappa_{AFP}} - 1 \leq 0 \end{aligned} \tag{11}$$

where the superscript i denotes the number of different plies within the laminate.

The range of the design variables is indicated in Table 1. Note that the fiber angles, T_0^i and T_1^i, will be multiplied by 90 and ε and α will be converted to x,y coordinates when the FE model is built.

Table 1: Range of the design variables

	T_0^i	T_1^i	ε	α
Lower bound	-1	-1	0	-1
Upper bound	1	1	0.25	1

In the present work, the following values of GA parameters have been chosen based on the author's experience as a compromise between the sufficient reliability of the optimal solution and a reasonable calculation price. A population size of 60 individuals is chosen to be ten times the number of design variables. The stopping criterion has been set at maximum of 60 generations.

3.1. Curvature Constraint

The design of composite panels with curvilinear fibers and curvilinear stiffeners should consider the limit allowed on the maximum curvature by the AFP machine. This manufacturing constraint is imposed to avoid local wrinkling when the tow is overly curved. According to [22], the curvature for the tow configuration chosen (course of 32 tows with a width of $3.175 \times 10^{-3}\,\mathrm{m}$) is limited to $k_{AFP} = 1.57\,\mathrm{m}^{-1}$.

The fiber path of the skin and stiffeners is 2D, therefore, the curvature definition for a planar function (Eq 12) is employed.

$$\kappa = \frac{y''}{(1 + (y')^2)^{3/2}} \tag{12}$$

Here below, it is explained how to compute the curvature, first for the skin fibers and then for the stiffener fibers.

3.1.1 Skin Fibers Curvature

In the shifted method, the fiber paths have identical orientation. The fiber path defined by the linear variation of the angle is antisymmetric. The above means that is only necessary to compute the curvature for the positive side of the reference fiber path.

The curvature of the skin fibers can be calculated by Eq.12, in which $y(x)$ stands for the fiber reference path. After a little algebra, the curvature is obtained in terms of T_1, T_0, $\theta(x)$ and a, as shown in Eq.13.

$$\kappa(x) = \frac{T_1 - T_0}{a} cos\theta(x) \tag{13}$$

The curvature has to be evaluated at x-positions. These x-positions correspond to the center of the (positive) x-divisions of the skin mesh. The maximum curvature of the fiber path, $\kappa^i_{max,f}$, is then obtained and compared to the maximum curvature of the AFP machine, κ_{AFP}. The absolute value is used since the curvature is a signed quantity. Note that there will be as many curvature constraints for the skin as different i layers of the laminate (Eq.14).

$$\frac{\left|\kappa^i_{max,f}\right|}{\kappa_{AFP}} - 1 \leq 0 \tag{14}$$

3.1.2 Stiffener curvature constraint

The stiffeners are modeled directly in Abaqus using the spline tool. To evaluate the curvature with Eq.12, it is necessary to know the analytical function of the spline. Abaqus calculates the shape of the curve using a cubic spline fit between all points along the spline [20].

The mathematical method to determine the cubic spline function can be found in reference [23] and is not described here for the shake of brevity.

Once the cubic spline function is obtained, it is possible to interpolate the value of an arbitrary point on the stiffener and compute its curvature. Note that the four stiffeners are equal, so the values of the curvature are only calculated for one of them. Next, the relative difference between the maximum curvature of the stiffener, $\kappa_{max,s}$, and the maximum curvature allowed by the AFP machine, κ_{AFP} is calculated and implemented as a constraint (Eq.15).

$$\frac{\kappa_{max,s}}{\kappa_{AFP}} - 1 \leq 0 \tag{15}$$

4. Results

4.1. Case Studies

In this study, a square composite panel of dimensions $2a \times 2a$ is optimized. The value of a is set to 0.5 m. Two stacking sequences are considered for the skin laminate: $\left[\left\langle T_0^1, T_1^1\right\rangle / \left\langle T_0^2, T_1^2\right\rangle\right]_s$ (laminate A) and $[\pm\left\langle T_0^1, T_1^1\right\rangle / \pm \left\langle T_0^2, T_1^2\right\rangle]_{2s}$ (laminate B). Each ply has a thickness, t_{ply}, of 1.27×10^{-4} m.

The thickness of the stiffener, t_s, is equal to that of the skin, t_p, i.e., both laminates have the same number of plies. The stiffener height, h_s, is set as five times the stiffener thickness. Therefore, the stiffener depth ratio, h_s/t_s, is 5, a value for which global or plate local buckling modes are expected [11]. The stiffener blade buckling is not considered. Figure 6 schematizes the panel to be optimized and indicates its dimensions.

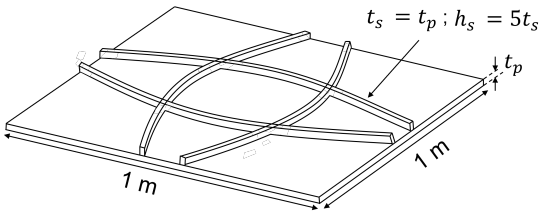

Figure 6: Scheme of the panel to be optimized

The parameters to define the tow course, which are the the tow width and the number of tows in a course, are set to $t_w = 3.175 \times 10^{-3}$ m and $n_t = 32$, respectively.

The material properties of both the skin and the stiffeners are given in Table 2. The properties of a generic epoxy resin, employed to fill the gaps, are also indicated in Table 2.

Table 2: Material properties

Graphite-Epoxi		Epoxi	
E_1	132.38 GPa		
E_2	10.76 GPa	E_m	3.7 GPa
E_3	10.76 GPa		
ν_{12}	0.24		
ν_{13}	0.24	ν_m	0.3
ν_{23}	0.49		
G_{12}	5.65 GPa		
G_{13}	5.65 GPa	G_m	1.4 GPa
G_{23}	3.38 GPa		

When panels with gaps are optimized, Poisson's ratios are assumed equal ($\nu_{12} = \nu_{13} = \nu_{23}$) because a rule of mixture for ν_{23} has not been stated.

Certain boundary conditions and load cases have been selected to represent what a wing panel of an aircraft may experience. The three different boundary conditions addressed are the following. All plate edges are simply supported (SSSS). Two plate edges are simply supported at $y = -a, y = a$ and the other two are clamped at $x = -a, x = a$ (SSCC). All plate edges are clamped (CCCC).

Here, for the simply supported boundary condition there is no out-of-plane displacement, i.e., $w = 0$. The clamped boundary condition restricts, in addition to the out-of-plane displacement, the rotations along the x-axis and y-axis, i.e., $w = \theta_x = \theta_y = 0$. In all cases, to avoid body solid rigid motion, the bottom left corner and bottom right corner are constrained to $v = 0$ and $u = v = 0$, respectively.

The two load cases considered are: biaxial compression load case and biaxial compression plus shear load. Figure 7 schematizes two possible combinations of load cases and boundary conditions.

The optimization results are compared to a constant stiffness composite panel with straight stiffeners. The stacking sequence $[\pm 45/0/90]$ is used for comparison with laminate A and $[\pm 45/0/90]_{2s}$ for laminate B. The straight stiffeners are placed equidistant from each other.

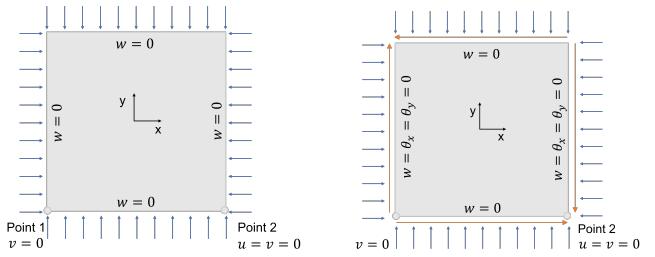

(a) Biaxial compression & SSSS

(b) Biaxial compression plus Shear & SSCC

Figure 7: Two combinations of load cases and boundary conditions

The critical buckling load has been obtained for all load cases and boundary conditions. For brevity, the results are not shown, but the percent improvement of the curvilinear fiber panels with respect to the straight fiber analogues will be indicated.

4.2. Biaxial compression load case

Four case studies have been optimized for ideal VS panels with curvilinear stiffeners, subjected to biaxial compressive load: the first one with laminate A (4 plies) and SSSS boundary conditions, the other three with laminate B (16 plies) and boundary conditions of SSSS; SSCC; CCCC. The same case studies have been also optimized considering the gap effect.

Table 3 indicates the results of the optimization: the value of the design variables, the maximum curvature for ply 1 (k_1), ply 2 (k_2) and stiffeners (k_s), the critical buckling load, and the improvement with respect to the straight fiber design. The configuration for ply 1, ply 2, the stiffener layout, and the first buckling mode for each of the four case studies are shown in Figure 8. The results for panels with gaps are provided in Table 4 and Figure 9. Table 4 also gives the average gap area encountered for a ply of the laminate. It is calculated as the sum of the gap area in each ply divided by the total laminate area.

A glance at the tables and figures mentioned shows that for the SSSS boundary condition, the fiber angles of ply 1 and ply 2 are comparable in both ideal panels and panels with gaps. The stiffener layout also presents a similarity for both scenarios. The maximum curvatures of the skin and stiffener fibers are near or at the maximum allowable curvature, taking full advantage of the tow steering capability. Although the gaps formed in VS laminates deteriorate the buckling performance, the average gap area for the optimized panels is not much higher than 2%. Therefore, the critical load has not decreased significantly. For panels with embedded gaps, the buckling load is 145 N/m if laminate A is optimized, and 24 190 N/m if it is laminate B. The difference between the two buckling loads is because the number of total plies involves both the laminate thickness and the dimensions of the stiffener blade. The panel buckles in a global manner for all scenarios here. The improvement in buckling load for panels considering gaps with respect

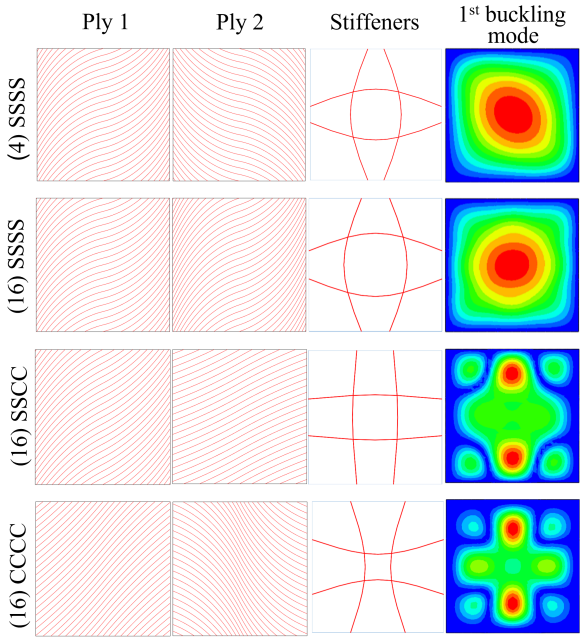

Figure 8: Optimized ideal panels subjected to biaxial compression

to the straight fiber counterparts is 51% for laminate A and 40% for laminate B.

A different behaviour is encountered with the SSCC boundary condition. The skin fibers show considerable curvature, but far from the maximum permitted. The average gap area is 1.76%, which is lower than in cases where the skin fibers reach the maximum curvature. The stiffeners are of very low curvature.The two clamped edges have implied a significant increase in buckling load and a change in the buckling mode shape with respect to the SSSS case. Now the the panel buckles locally with the buckle peaks at the top and bottom edges. For optimized panels with embedded gaps, the buckling load has a value of 41 010 N/m. The improvement with respect to the straight fiber analogue is 14%, mainly due to the skin curvilinear fibers, since the stiffener layout is almost equal to the straight configuration. In this case, the possibility of curving the stiffener fibers has not revealed a substantial advantage in the panel buckling performance.

In the last boundary condition (CCCC), the fibers of one of the plies do not show a high curvature while the fibers of the other ply are significantly curved. The stiffeners curve significantly towards the center of the panel. The optimum panel considering gaps presents an average percent area of 1.86%. The resulting buckling load is 49 360 N/m for the panel with gaps. The panel buckles in a local manner. The improvement compared to the straight fiber design is 23%.

4.3. Biaxial Compression plus Shear load case

The results of the optimization for ideal panels subjected to biaxial compression plus in-plane shear are presented in Table 5 and Figure 10. The results when gaps are considered are given in Table 6 and Figure 11. In this load

Table 3: Optimization results of ideal panels subjected to a biaxial compression load

Total plies	Boundary Conditions	T_0^1 (°)	T_1^1 (°)	T_0^2 (°)	T_1^2 (°)	ε	α	Max Curvature $[m^{-1}]$	Buckling Load $[N/m]$	Improvement (%)
4	SSSS	14.2	60.9	-11.6	-57.8	0.110	0.387	$\kappa_1 = 1.57$ $\kappa_2 = 1.57$ $\kappa_s = 1.57$	150	57
16	SSSS	13.9	59.5	18.5	66.2	0.0987	0.475	$\kappa_1 = 1.54$ $\kappa_2 = 1.57$ $\kappa_s = 1.57$	24210	40
16	SSCC	27.5	56	29.3	20.4	0.159	-0.337	$\kappa_1 = 0.876$ $\kappa_2 = 0.289$ $\kappa_s = 0.377$	41360	15
16	CCCC	50.2	38.9	-62.1	-21.6	0.177	-0.193	$\kappa_1 = 0.305$ $\kappa_2 = 1.30$ $\kappa_s = 1.32$	49770	24

Table 4: Optimization results of panels considering gap effect, subjected to biaxial compression load

Total plies	Boundary Conditions	T_0^1 (°)	T_1^1 (°)	T_0^2 (°)	T_1^2 (°)	ε	α	Max Curvature $[m^{-1}]$	Gap Area (%)	Buckling Load $[N/m]$	Improvement (%)
4	SSSS	15.4	60.7	-9	-54.6	0.138	-0.364	$\kappa_1 = 1.51$ $\kappa_2 = 1.55$ $\kappa_s = 1.57$	2.03	145	51
16	SSSS	15.6	57.4	-15.6	-62.2	0.104	0.433	$\kappa_1 = 1.40$ $\kappa_2 = 1.55$ $\kappa_2 = 1.57$	2.07	24190	40
16	SSCC	34	23.6	-20	-50.4	0.160	-0.280	$\kappa_1 = 0.333$ $\kappa_2 = 0.990$ $\kappa_s = 0.018$	1.76	41010	14
16	CCCC	55.2	21	-38.8	-56.6	0.183	-0.197	$\kappa_1 = 1.11$ $\kappa_2 = 0.481$ $\kappa_s = 1.57$	1.86	49360	23

case, the laminate A (4 plies) has not been optimized.

This load case presents a similar pattern to that of the biaxial compression. For the SSSS boundary case, high values of curvature near or at the limit of the maximum curvature for both plies and stiffener fibers are obtained. The average gap area is 2.08%. The buckling load for the panel with gaps is 40 870 N/m and the buckling shape is of global nature. The improvement with respect to the straight fiber counterpart is 26%.

In the case of SSCC boundary condition, the fibers of ply 1 exhibit an important curvature and the fibers of ply 2 are close to the maximum curvature. By contrast, the stiffeners are of very low curvature. The average gap area has a value of 1.97%. For the panel considering the gap effect, the buckling load achieved is 69 010 N/m. The improvement over the straight fiber design is 12%. This modest value is mostly due to the skin fiber curvature, as almost straight stiffeners are preferred under SSCC case.

For the CCCC boundary condition case, the skin fibers are considerably curved. The average gap area is 2.26%, the highest value of all optimized cases. It is because the high value of T_0 in ply 1 leads to increased gap formation. The stiffeners show moderate curvature. The buckling load of the panel with gaps is 81 450 N/m and the buckling mode is local. The resulting improvement compared to the straight fiber design is 16%.

5. Conclusions

In this work, a framework has been developed to optimize the buckling performance of composite panels with curvilinear fibers and curvilinear grid stiffeners. The manufacturing aspects of the AFP machine have been considered in the design phase. The maximum curvature allowed by the AFP machine has been imposed on both the skin and stiffener fibers. The effect of the gaps formed when manufacturing VS laminates has been also incorporated.

Different load cases and boundary conditions have been studied. It has been observed that in all cases the skin fibers have shown curvature. Depending on the boundary conditions, the skin fiber curvature is different, being in some cases the maximum allowed and in others a moderate value. It was observed that the manufacturing-induced gaps in VS laminates worsened the buckling performance of the panel. Since the optimized panels presented a low gap area, the buckling load did not excessively decreased compared to the ideal panels. Curvilinear skin fibers that induce gaps were preferred to straight fibers that do not cause gaps.

As for the grid layout, the stiffeners were generally located in intermediate positions neither near the center nor near the edges of the panel. The stiffeners exhibited

Table 5: Optimization results of ideal panels subjected to biaxial compression plus shear load

Total plies	Boundary Conditions	T_0^1 (°)	T_1^1 (°)	T_0^2 (°)	T_1^2 (°)	ε	α	Max Curvature $[m^{-1}]$	Buckling Load $[N/m]$	Improvement (%)
16	SSSS	20.2	55.0	17.3	63.1	0.100	0.464	$\kappa_1 = 1.13$ $\kappa_2 = 1.51$ $\kappa_s = 1.57$	41000	27
16	SSCC	37.9	11.2	16.1	63.0	0.169	-0.311	$\kappa_1 = 0.913$ $\kappa_2 = 1.57$ $\kappa_s = 0.249$	69050	12
16	CCCC	36.2	23.9	20.3	68.7	0.0976	0.353	$\kappa_1 = 0.390$ $\kappa_2 = 1.57$ $\kappa_s = 0.790$	85620	22

Table 6: Optimization results of panels considering gap effect, subjected to biaxial compression plus shear load

Total plies	Boundary Conditions	T_0^1 (°)	T_1^1 (°)	T_0^2 (°)	T_1^2 (°)	ε	α	Max Curvature $[m^{-1}]$	Gap Area (%)	Buckling Load $[N/m]$	Improvement (%)
16	SSSS	15.9	61	-13.6	-60.2	0.0949	0.488	$\kappa_1 = 1.50$ $\kappa_2 = 1.57$ $\kappa_s = 1.47$	2.08	40870	26
16	SSCC	42.4	10.4	16.8	62.4	0.161	-0.295	$\kappa_1 = 1.09$ $\kappa_2 = 1.51$ $\kappa_s = 0.052$	1.97	69010	12
16	CCCC	72.7	36.2	26.3	64.2	0.099	0.322	$\kappa_1 = 1.01$ $\kappa_2 = 1.17$ $\kappa_s = 0.665$	2.26	81450	16

a high or even the maximum allowable curvature when SSSS and CCCC boundary conditions were optimized. For the SSCC case, quasi-straight stiffeners were preferred. Under this boundary condition, curvilinear stiffeners did not demonstrate a major advantage in panel buckling behavior.

It was shown that the use of curvilinear fibers for both skin and stiffeners can enhance the buckling performance. However, depending on the load case and boundary conditions, there might not be a significant improvement compared to the straight fiber counterpart. The optimization framework developed could help the designer to evaluate in which scenarios composite panels with curvilinear fibers and grid stiffeners provide the greatest benefit. To that end, load cases and boundary conditions different from those covered here should be studied. Other dimensions of the skin and stiffeners could also be considered.

The design space could be expanded by optimizing the thickness and height of the stiffeners or defining different stiffener layouts. Several reference paths for the skin laminate could be implemented to fully explore the tailoring capability of curvilinear fibers. The number of tows, the tow width, and the coverage percentage affect the gap and/or overlap distribution in VS layers. Studies varying these manufacturing parameters could be conducted to investigate their effect on buckling behavior. The panels could be modeled with a slight curvature to more closely resemble the wing and fuselage skins of the aircraft. Post-buckling behavior and experimental testing of VS panels with curvilinear stiffeners could constitute areas of future research.

References

[1] R.Olmedo and Z.Gurdal. Buckling response of laminates with spatially varying fiber orientations. *Collection of Technical Papers - AIAA/ASME Structures, Structural Dynamics and Materials Conference*, pages 2261–2269, 1993. doi:10.2514/6.1993-1567.

[2] Z.Wu, P.Weaver, G.Raju, and B.Kim. Buckling analysis and optimisation of variable angle tow composite plates. *Thin-Walled Structures*, 60:163–172, 2012. doi:10.1016/j.tws.2012.07.008.

[3] S.Ijsselmuiden. *Optimal design of variable stiffness composite structures using lamination parameters*. PhD thesis, Delft University of Technology, 2011.

[4] A.Blom, C.Lopes, P.Kromwijk, Z.Gurdal, and P.P.Camanho. A theoretical model to study the influence of tow-drop areas on the stiffness and strength of variable-stiffness laminates. *Journal of Composite Materials*, 43(5):403–425, 2009. doi:10.1177/0021998308097675.

[5] K.Fayazbakhsh, M.Arian Nik, D.Pasini, and L.Lessard. Defect layer method to capture effect of gaps and overlaps in variable stiffness laminates made by automated fiber placement. *Composite Structures*, 97:245–251, 2013. doi:10.1016/j.compstruct.2012.10.031.

[6] T.Brooks and J.Martins. On manufacturing constraints for tow-steered composite design optimization. *Composite Structures*, 204:548–559, 2018. doi:10.1016/j.compstruct.2018.07.100.

[7] A.Alhajahmad and C. Mittelstedt. Buckling performance of curvilinearly grid-stiffened tow-placed composite panels considering manufacturing constraints. *Composite Structures*, 260:113271, September 2021. doi:10.1016/j.compstruct.2020.113271.

[8] D.Liu, P.Hao, K.Zhang, K.Tian, B.Wang, G.Li, and W.Xu. On the integrated design of curvilinearly grid-stiffened panel with non-uniform distribution and variable

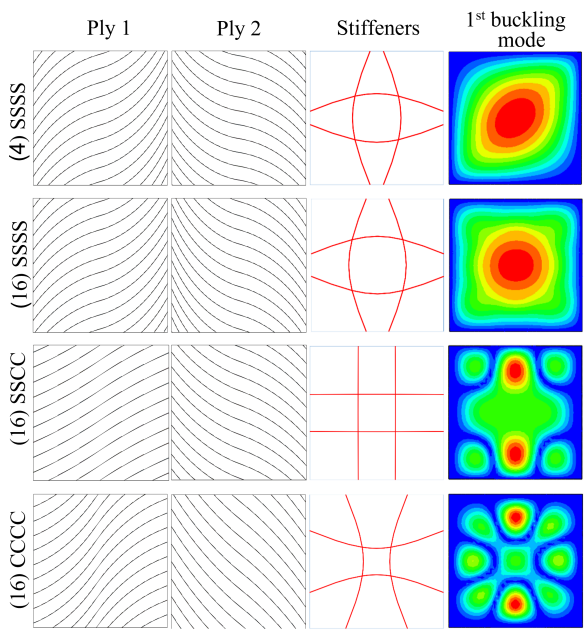

Figure 9: Optimized panels considering gap effect, subjected to biaxial compression

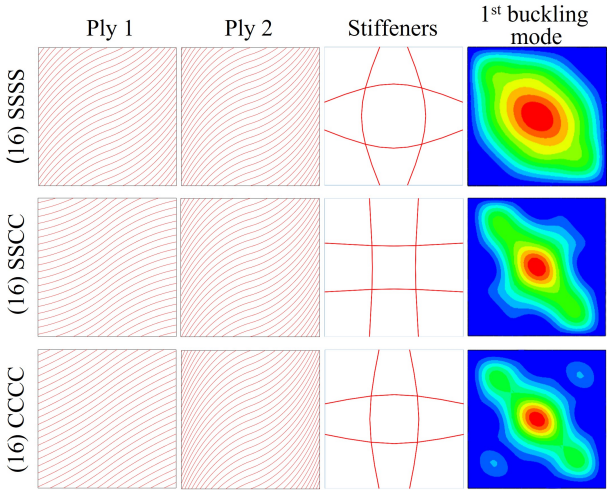

Figure 10: Optimized ideal panels subjected to biaxial compression plus shear

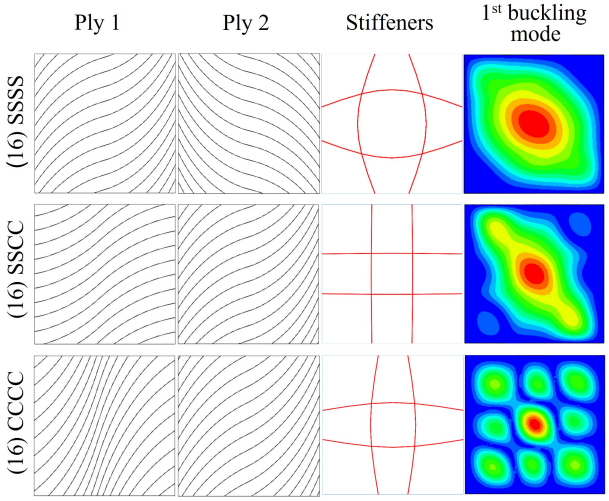

Figure 11: Optimized panels considering gap effect, subjected to biaxial compression plus shear

stiffener profile. *Materials and Design*, 190:108556, 2020. doi:10.1016/j.matdes.2020.108556.

[9] D.Wang, M.Abdalla, and W.Zhang. Buckling optimization design of curved stiffeners for grid-stiffened composite structures. *Composite Structures*, 159:656–666, 2017. doi:10.1016/j.compstruct.2016.10.013.

[10] L.Praticò, J.Galos, E.Cestino, G.Frulla, and P.Marzocca. Experimental and numerical vibration analysis of plates with curvilinear sub-stiffeners. *Engineering Structures*, 209:109956, 2020. doi:10.1016/j.engstruct.2019.109956.

[11] W.Zhao and R.Kapania. Buckling analysis of unitized curvilinearly stiffened composite panels. *Composite Structures*, 135:365–382, 2016. doi:10.1016/j.compstruct.2015.09.041.

[12] R.Kapania, J.Li, and H.Kapoor. Optimal design of unitized panels with curvilinear stiffeners. *Collection of Technical Papers - AIAA 5th ATIO and the AIAA 16th Lighter-than-Air Systems Technology Conference and Balloon Systems*, 3:1708–1737, 2005. doi:10.2514/6.2005-7482.

[13] K.Singh and R.Kapania. Buckling load maximization of curvilinearly stiffened tow-steered laminates. *Journal of Aircraft*, 56:2272–2284, 2019. doi:10.2514/1.C035358.

[14] R.Vescovini, V.Oliveri, D.Pizzi, L.Dozio, and P.Weaver. Prebuckling and buckling analysis of variable-stiffness, curvilinearly stiffened panels. *Aerotecnica Missili & Spazio*, 99:43–52, 2020. doi:10.1007/s42496-019-00031-4.

[15] T.Dang, K.Kapania, W.Slemp, M.Bhatia, and S.Gurav. Optimization and postbuckling analysis of curvilinear-stiffened panels under multiple-load cases. *Journal of Aircraft*, 47:1656–1671, 2010. doi:10.2514/1.C000249.

[16] S.Nagendra, R.T. Haftka, and z.Gürdal. Design of a blade stiffened composite panel by a genetic algorithm. *Collection of Technical Papers - AIAA/ASME Structures, Structural Dynamics and Materials Conference*, pages 2418–2436, 1993.

[17] P.Hao, C. Liu, X.Yuan, B.Wang, G.Li, T.Zhu, and F.Niu. Buckling optimization of variable-stiffness composite panels based on flow field function. *Composite Structures*, 181:240–255, 2017. doi:10.1016/j.compstruct.2017.08.081.

[18] B.Tatting and Z.Gürdal. Design and manufacture tow placed plates of elastically tailored. *NASA/CR*, 2002.

[19] C.Waldhart. Analysis of tow-placed, variable-stiffness laminates. Master's thesis, Faculty of the Virginia Polytechnic Institute and State University, 1996.

[20] Dassault Systemes. *Abaqus 6.14 Documentation*, 2014. http://130.149.89.49:2080/v6.14/.

[21] W.Zhao and R.Kapania. Vibration analysis of curvilinearly stiffened composite panel subjected to in-plane loads. *AIAA Journal*, 55(3):981–997, 2017. doi:10.2514/1.J055047.

[22] A.W.Blom. *Structural performance of fiber-placed, variable-stiffness composite conical and cylindrical shells*. PhD thesis, Delft University of Technology, 2010.

[23] J.Kiusalass. *Numerical Methods in Engineering with MATLAB*, chapter 3. Cambridge University Press, second edition, 2010.